PHILOSOPHICAL TRANSACTIONS OF THE ROYAL SOCIETY B BIOLOGICAL SCIENCES

Simulation of Late Permian Climate and Biomes with an Atmosphere-Ocean Model: Comparisons with Observations

J. E. Kutzbach and A.M. Ziegler

Phil. Trans. R. Soc. Lond. B 1993 **341**, 327-340
doi: 10.1098/rstb.1993.0118

Simulation of Late Permian climate and biomes with an atmosphere–ocean model: comparisons with observations

J. E. KUTZBACH[1] AND A.M. ZIEGLER[2]

[1]*Center for Climatic Research, University of Wisconsin-Madison, 1225 West Dayton Street, Madison, Wisconsin 53706, U.S.A.*

[2]*Department of Geophysical Sciences, University of Chicago, 5734 S. Ellis, Chicago, Illinois 60637, U.S.A.*

SUMMARY

A climate model is used to simulate the climate of the Late Permian. The climate model employs more detailed prescriptions of land–ocean boundaries, topography, and inland lakes and seas than were used in previous climate simulations of supercontinents with idealized land–ocean boundaries and no topography. The presence of mountains and plateaus and of inland seas and lakes produce large differences in the simulated climate compared to simulations that omit these features. Mountains and plateaus become focal points for enhanced precipitation and also help to intensify the monsoon circulations. Extensive inland seas and lakes exert a strong local damping of the seasonal range of temperature and also cause changes beyond the lakes region due to dynamical and hydrological effects. Using the climate–biome classification scheme of Walter, the simulated distribution of climates–biomes is compared to the observed distribution of Late Permian vegetation–biomes. Agreement is good in all but two areas.

1. INTRODUCTION

Experiments with climate models have demonstrated that supercontinents, such as existed in the Late Permian, must have experienced large seasonal temperature extremes (Crowley *et al.* 1987) and strong monsoons, with heavy rains along tropical coasts but arid interiors (Kutzbach & Gallimore 1989). Large seasonal temperature extremes are expected because large fractions of the huge landmass are far removed from the moderating influence of the surrounding oceans. This situation might be similar to, but more extreme than, the hot summers and cold winters of central Asia today. Similarly, the interior of a supercontinent should be arid because the oceanic moisture sources are so far removed. Moist climates or seasonally moist climates are expected only along tropical coasts, where strong monsoonal wind circulations dominate, and in middle and high latitudes where strong westerly flow advects moisture inland (Kutzbach & Gallimore 1989). While geographic controls on climate are very important, the roles of topography and the fainter sun and altered greenhouse gas concentration of late Palaeozoic time need also to be considered in estimating the palaeoclimate (Crowley & Baum 1992; Kutzbach & Gallimore 1989).

The purpose of this paper is: (i) to report results of two simulations for the Late Permian (Kazanian), about 250 Ma BP, in which geography, topography, and, in one experiment, inland seas and lakes have been specified in considerable detail; and (ii) to compare the simulated climate, as expressed in terms of modern-day climates–biomes, with botanical evidence from the Late Permian (Ziegler 1990). Both simulations use more realistic land–ocean distributions and include estimates of topography, in contrast to previous simulations with idealized geography and no mountains (Kutzbach 1994; Kutzbach & Gallimore 1989). By comparing these new simulations with the previous simulations, we can assess the importance of these changes in geography and topography. The two Late Permian simulations described in this paper differ in that one includes large inland seas and waterways in Gondwana, as described by Yemane (1993) and Ziegler (1993). These authors have argued that the failure of climate modelers to include these lakes and seas in models may be a major factor in understanding why simulations of the climate of supercontinents have consistently exhibited extreme seasonality (very hot summers and very cold winters) whereas palaeobotanical data and other fossil records suggest a more temperate climate. By comparing these two simulations of Late Permian climate, one with extensive inland lakes and seas and one without, we can assess the sensitivity of the climate to the presence of large lakes and seas.

2. MODEL DESCRIPTION

The simulation experiments were made with the community climate model (CCM) of the National Center for Atmospheric Research (NCAR); see Ran-

Phil. Trans. R. Soc. Lond. B (1993) **341,** 327–340
Printed in Great Britain

del & Williamson (1990) for a description of version 1 of the model (CCM1). The model incorporates atmospheric dynamics based upon the equations of fluid motion; it includes radiative and convective processes, condensation, precipitation and evaporation. Surface energy and hydrologic budget equations permit the calculation of surface temperature, soil moisture, snow melt, and runoff. The version of the CCM1 used here was modified by Covey & Thompson (1989) to include a 50 m thick mixed layer ocean for calculating ocean temperature and sea ice thickness and location. The ocean has no explicit currents but includes, as a prescribed flux, the estimated poleward transport of heat by the oceans. The model has twelve vertical levels in the atmosphere and one ocean level, and uses a spectral waveform representation, to wavenumber 15 (R15), of the horizontal fields of wind, temperature, pressure and moisture. When needed for certain calculations the spectral representation is converted to a grid of 4.4° latitude by 7.5° longitude. The model simulates the entire seasonal cycle, January through December, with a time step of 30 min. The model was run for 20 years with the last five years being used for these analyses. The twenty years of calculation allowed the mixed-layer ocean and sea-ice distributions to reach quasi-equilibrium values in response to the imposed seasonal cycle of solar radiation.

The control case simulations of the current climate by the CCM have known shortcomings in comparison to observations (Randel & Williamson 1990), and these deficiencies may also have an effect on the model's sensitivity to orbital change. For example, the model's troposphere is colder, by several°C, than the observed atmosphere and has weaker mid-latitude westerlies and weaker subtropical easterlies than the observed atmosphere. The simulated transient disturbances, such as mid-latitude storms, are weaker than observed. On the other hand, the general patterns of large-scale circulation, temperature and precipitation are similar to observations (Pitcher *et al.* 1983). Because of the coarse spatial resolution of the model, the simulated boundaries separating warm–cold and wet–dry regions are not as sharply defined as the observed boundaries.

This model has several important differences compared to the model used in previous Pangean climate experiments (Kutzbach & Gallimore 1989): (i) the horizontal and vertical resolution of the model is significantly increased; (ii) the parameterizations for radiation, clouds, snow cover and vertical diffusion, processes which are important for the surface energy balance, are improved. An important limitation that remains in the model is the greatly oversimplified treatment of the ocean.

3. EXPERIMENTAL DESIGN

A number of internal and external boundary conditions are prescribed for the late Permian including: land–ocean distribution, topography, land surface albedo, ocean heat flux, solar irradiance, orbital parameters, and atmospheric CO_2 concentration.

The land–ocean distribution (figure 1*a*) for Late Permian time (the Kazanian), is taken from Ziegler (1990, figure 4). The model grid for specifying geographic features is 4.4° of latitude by 7.5° longitude and therefore features smaller than these grid squares are not resolved. The land–ocean distribution in our second experiment (figure 1*b*) is modified to include large inland seas and lakes as described by (Yemane 1993). Most of these seas and lakes are either smaller than the 4.4° by 7.5° model grid boxes, or occupy fractions of two grid boxes. In our attempt to assess the possible importance of these inland waters we have overestimated their spatial extent somewhat. The depth of the inland waters is set at 50 m, the same as ocean grid boxes.

The topography (figure 1*a*) is estimated from maps of (Ziegler 1990, figure 4). The relatively coarse spatial resolution of the model prevents accurate representation of topographic features. For example, narrow and high mountains are represented as relatively broad and low. In this simulation, large mountains and plateaus are located along an east–west line to the north of the equator (maximum elevation 2300 m), along the west coast of Gondwana (2100 m), and in central and eastern Laurasia (1400 m). The average elevation of the land above sea level is 480 m, compared to 680 m in the control simulation with present-day topography. Because of the model's relatively coarse spatial resolution, the topography in the vicinity of the Southern Hemisphere lakes (figure 1*b*) is very similar to that in the simulation without southern lakes (figure 1*a*).

The land surface albedo is prescribed at values ranging from about 0.13 to about 0.24. The vegetation biome maps for the Kazanian (Ziegler 1990, figure 4) were used to assign relatively low albedo (0.13 to 0.17) to well-vegetated regions, and relatively high albedo (0.18 to 0.24) to poorly vegetated regions or deserts. In future experiments, it will be desirable to use an interactive vegetation model to avoid prescribing the land albedo and thereby possibly biasing the regional climate toward a particular result.

There is no accurate means of estimating ocean heat flux for the Late Permian. We have used zonal-average values of ocean heat flux obtained from a simulation of an idealized ocean for Pangean time driven by winds and surface temperature from a previous atmospheric simulation (Kutzbach *et al.* 1990). Using this approach, the model extracts about 50 W m^{-2} from the equatorial oceans and returns this energy to the middle and high latitude oceans especially around 45–65° latitude. In this way, the model accomplishes a significant poleward heat transport (by ocean currents) that lowers tropical sea surface temperatures and raises polar temperatures.

Based upon models of stellar evolution (Crowley & North 1991) the solar irradiance for late Permian time is reduced by 1%, from the modern value of 1370 W m^{-2} to 1356 W m^{-2}. The Earth's orbit about the Sun is set to be circular and the axial tilt is set at the modern value of 23.5°.

There is great uncertainty about the concentration of carbon dioxide in the geologic past. Berner (1990) has estimated concentrations as large as 15 times

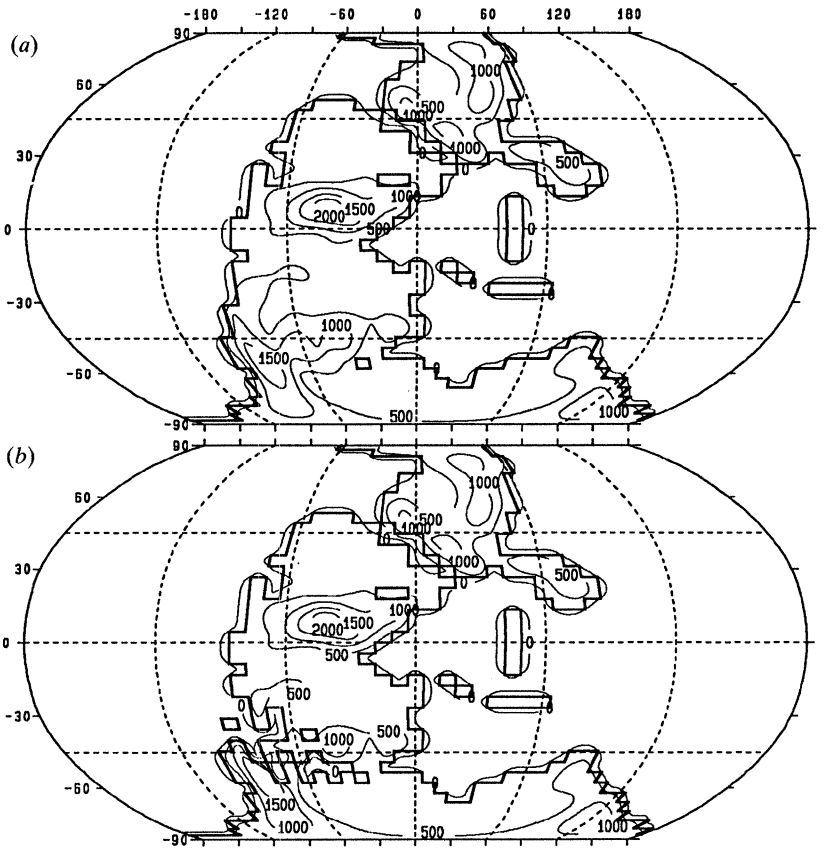

Figure 1. (*a*) Land–ocean distribution for the Late Permian, for simulation LP as represented on the coarse grid of the climate model. Topography is shown with 500 m contours. (*b*) As (*a*) except for the addition of extensive seas and lakes on the southern continent, simulation LP/EL.

present levels in the mid Palaeozoic and 5 times present levels in the mid Mesozoic. For the Late Permian, Berner's model estimates that CO_2 concentration was about 3 times the present level, with the range of uncertainty, based only on model sensitivity studies, being between about 2 and 5 times present. We have chosen to use a value of 5 times present concentration for this experiment. If this choice is too high, then our simulation will be biased toward warmer conditions, especially in the polar regions.

Analyses of growth increments on marine organisms, such as corals, bivalves and stromatolites, indicate that the Earth's rotation rate may have been about 5% faster than present during the Late Permian (Scrutton 1978) . While large changes in rotation rate would have a major impact on atmospheric circulation (Hunt 1979; Williams 1985), this relatively small change in rotation rate would not be expected to have a major effect on the climate and has not been included in our model simulation.

4. LATE PERMIAN CLIMATE SIMULATION

In this section, we describe the results of the two simulation experiments. We will refer to these experiments as: (i) Late Permian (LP) and (ii) Late Permian with extensive lakes (LP/EL). We summarize the results for surface temperature, sea-level pressure and surface winds, precipitation, and other indicators of the hydrologic budget. We will emphasize the seasonal extremes: June–July–August (JJA), and December–January–February (DJF).

(*a*) *The Late Permian (LP)*

Surface temperature exceeds 40–50°C in summer and falls below −15°C in winter in both hemispheres (figure 2*a*,*d*). The extremes, both high and low, are largest on the southern continent, which is larger than the northern continent. This fundamental relation between continent size and the degree of seasonality exits because the moderating effect of the ocean on the temperature of the continental interior decreases as the size of the continent increases (Crowley *et al.* 1986). Temperature extremes in central Laurasia are moderated by the presence of inland seas. Temperatures are also lower at higher elevations. Ocean temperature exceeds 30°C throughout the tropics and falls below 0°C only at high southern latitudes.

The distribution of sea-level pressure on the continents follows closely the seasonal swings of land surface temperature, with low pressure in summer and high pressure in winter (figure 3*a*,*c*) and with the most extreme values, i.e. the strongest summer and winter monsoons, over the larger southern continent. Strong monsoon winds blow from ocean to the southern continent in DJF (southern summer) and from ocean to the northern continent in JJA (northern summer).

PHILOSOPHICAL TRANSACTIONS OF THE ROYAL SOCIETY B BIOLOGICAL SCIENCES

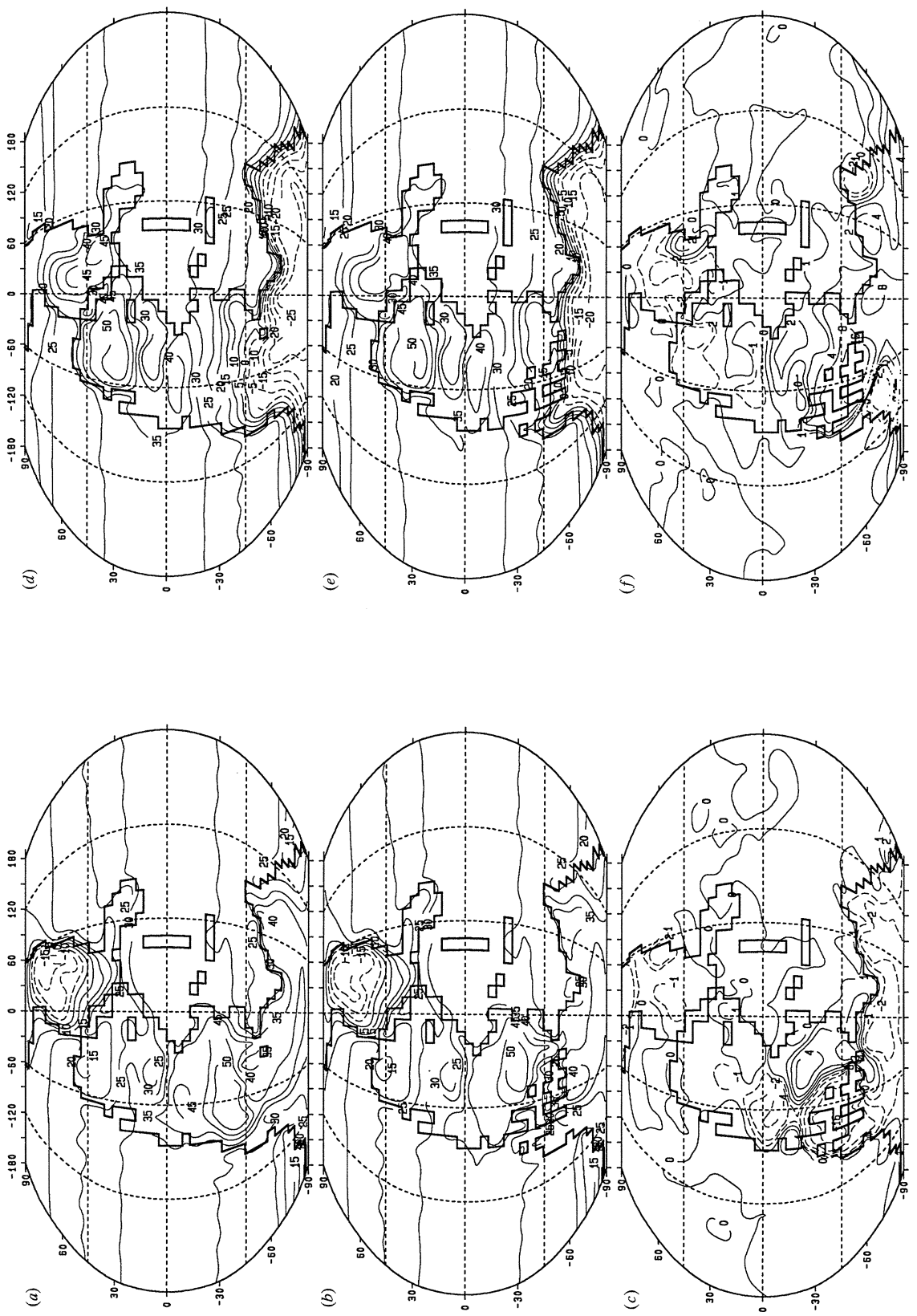

Figure 2. Surface temperature (°C) for December–January–February (DJF) for (*a*) simulation LP, (*b*) simulation LP/EL, and (*c*) the difference, LP/EL minus LP. (*d*,*e*,*f*) As (*a*,*b*,*c*) except for June–July–August (JJA).

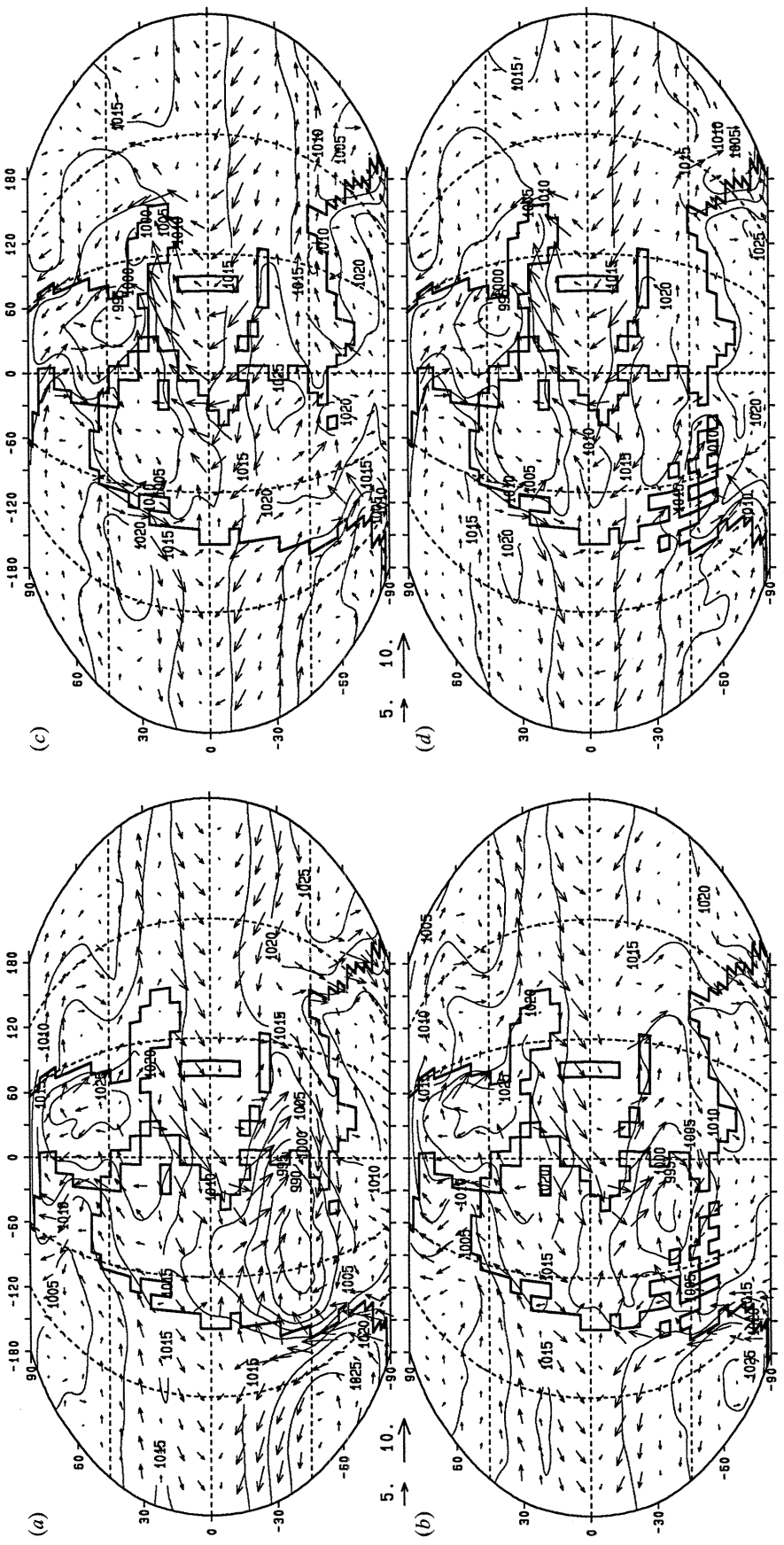

Figure 3. Sea level pressure (mb) and surface winds (m s^{-1}, see scaled arrows) for December–January–February (DJF) for (*a*) simulation LP, and (*b*) simulation LP/EL. Wind arrows are plotted at alternate latitudes and longitudes. Actual density of wind arrows is four times the plotted density. (*c*,*d*) As (*a*,*b*) except for June–July–August (JJA).

PHILOSOPHICAL TRANSACTIONS OF THE ROYAL SOCIETY B BIOLOGICAL SCIENCES

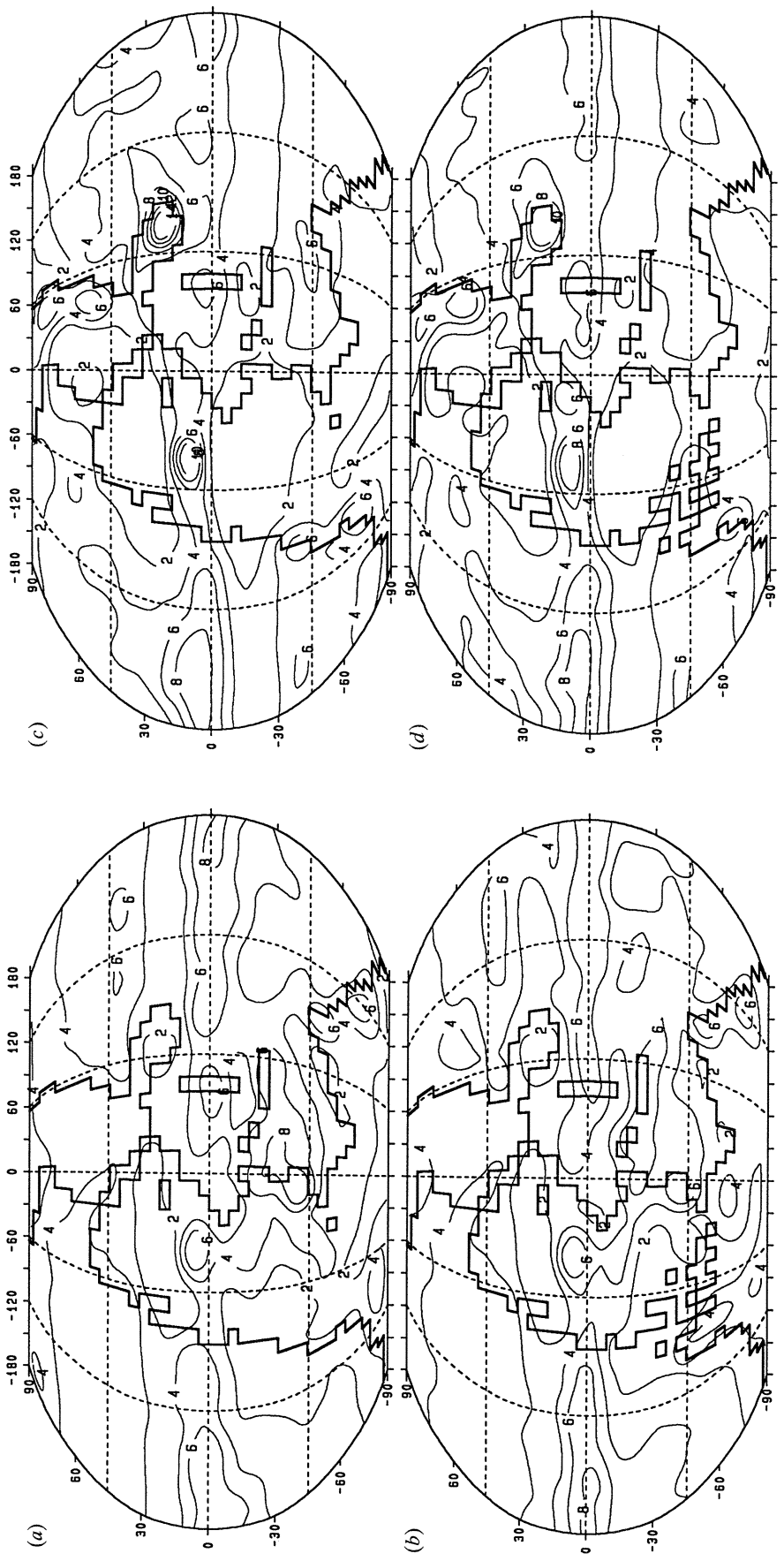

Figure 4. Precipitation (mm d^{-1}) for December–January–February (DJF) for (*a*) simulation LP, and (*b*) simulation LP/EL. (*c*,*d*) As (*a*,*b*) except for June–July–August (JJA).

PHILOSOPHICAL TRANSACTIONS OF THE ROYAL SOCIETY B BIOLOGICAL SCIENCES

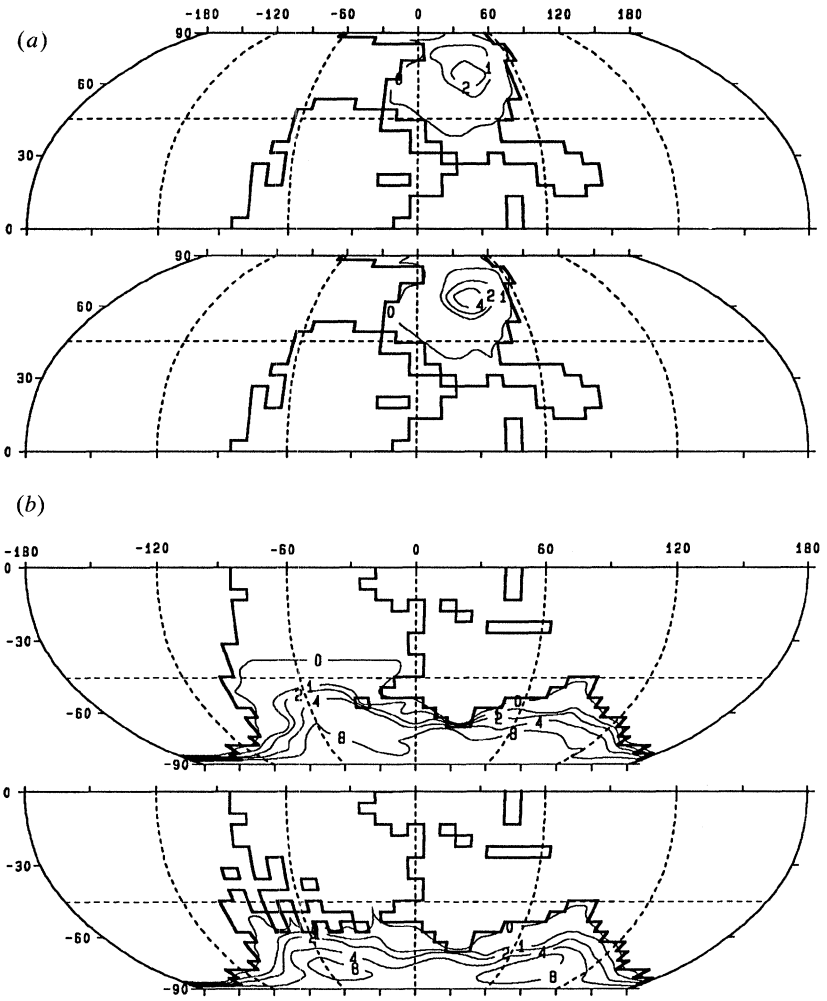

Figure 5. Water equivalent snow depth (cm) for (*a*) December–January–February (DJF), northern winter, and (*b*) June–July–August (JJA), southern winter; simulations for each hemisphere are LP (top) and LP/EL (bottom). One cm of water equivalent snow corresponds approximately to 10 cm of snow.

The topographic features included in the simulation influence the location of the centres of lowest pressure; these centres, near 40°S in DJF and near 40°N in JJA, are found in the vicinity of the subtropical–mid-latitude highlands. Especially in the southern summer, the presence of the western highlands causes the monsoon low to be centred farther west than in simulations for idealized continents with no topographic features (Kutzbach 1994). In the northern summer, the seaway through Laurasia helps to split the summer monsoon low pressure centre into two centres: the strong low located near 40°N over the highland of eastern Laurasia (mentioned above) and a weak secondary low located near 30°N in west central Laurasia (figure 3*c*).

Summer monsoon precipitation of 6–8 mm d^{-1} occurs along tropical and mid-latitude east coasts and near the north equatorial mountain range where upslope motions prevail in both DJF and JJA (figure 4*a*,*c*). Snow (figure 5) covers the northern part of Laurasia in DJF and Gondwana poleward of about 45°S in JJA, however, the snow melts each spring so there are no permanent snowfields. Sea ice (not shown) is restricted to high southern latitudes (poleward of 80°S) in southern winter.

(*b*) *Late Permian with extensive lakes (LP/EL)*

The presence of the extensive lakes and seas on the southern continent has a strong influence on the surface temperature in southern summer (figure 2*b*). Maximum temperatures in the lakes region are 25–30°C, similar to the ocean surface temperature at the same latitude, rather than 40–45°C (figure 2*a*). The temperature is 8–16°C lower in LP/EL, compared with LP, over the entire lake region (figure 2*c*). The region to the north and east of the lakes is somewhat warmer in LP/EL, compared with LP, due to changes in the monsoon circulation and the hydrologic cycle (see below). In southern winter, freezing temperatures are confined to the area south of the lake region (around 60°S) in LP/EL (figure 2*e*) whereas the zero degree isotherm extends to 45°S in LP (figure 2*d*). Southern winters are 8–16°C warmer in LP/EL than in LP (figure 2*f*). This wintertime warming extends eastward from the lakes region due to dynamical effects (see below). In summary, the seasonal extremes at around 45°S range from 45°C to −5°C in LP and from 30°C to 10°C in LP/EL. The lakes and seas reduce the seasonal range from 50°C (LP) to 20°C (LP/EL).

The large differences in surface temperature between the two simulations are associated with differences in low-level heating of the atmosphere. These differences in low-level heating produce dynamical responses that alter the atmospheric circulation in a manner consistent with theoretical studies by Hoskins & Karoly (1981). In southern summer, the low-level cooling over the lake region in LP/EL, realtive to LP, produces a low-level anticyclone over and downstream of the lakes in the sea-level pressure difference field (LP/EL minus LP; not shown). As a result, the southern summer monsoon low is less intense in LP/EL than in LP and is shifted to the east of the lake region (figure 3*a*,*b*). This change in the intensity and location of the low pressure centre reduces the penetration of moist tropical air into the interior and leads to reduced rainfall over and to the north and east of the lake region in LP/EL compared to LP (figure 4*a*,*b*). The reduced rainfall and associated reduction in evaporation and cloud cover cause the warming in surface temperature noted above (figure 2*c*). In southern winter, the increased low-level heating over the lake region in LP/EL, relative to LP, produces a low-level cyclone over and to the east of the lakes in the sea-level pressure difference field (not shown). As a result, there is a weak low pressure centre and a cyclonic circulation over the lake region (figure 3*d*), increased warmth to the east of the lake region (figure 2*f*) produced by the poleward flow on the eastern flank of the cyclonic circulation, and increased precipitation (figure 4*d*). Snow cover is less extensive in LP/EL, compared with LP, owing to the warmer winters in the lake region (figure 5).

(*c*) *Annual average conditions (LP/EL)*

The annual temperature for the two simulations are nearly identical except in the vicinity of the southern lakes. The net effect of the southern lakes is to cool the climate in the western region (where the effect of cooler summers dominates) and to warm the climate in the central and east region (where the effect of warmer winters dominates); see figure 6*a*,*b*. The annual precipitation exceeds 4 mm d^{-1} (1500 mm a^{-1}) in east coast summer monsoon regions and over the north equatorial east–west mountain range where upslope motion and precipitation occurs in all four seasons (figure 7). This broad east–west belt of high topographically forced precipitation is in marked contrast to the arid conditions found in the tropical interior in experiments without mountains (Kutzbach & Gallimore 1989; Kutzbach 1994). Precipitation also exceeds 1500 mm a^{-1} along the southern mid-latitude west coast where storm track precipitation occurs in fall, winter, and spring. The upslope motion along the coastal ranges of both southern and northern continents enhances the precipitation compared to previous experiments with no topography. The annual average soil moisture (figure 8) clearly delineates the arid regions of the subtropical continental interiors and the moist regions of the monsoon-dominated east coasts and the mid-latitude and high latitude regions influenced by the westerly storm tracks. The region of high soil moisture north of the equator coincides with the region of upslope precipitation associated with the large east–west mountain range.

(*d*) *Comparison with previous experiments*

The general features of both the LP and LP/EL simulations agree with those of previous simulations for more idealized 'box-shaped' Pangean continents (Kutzbach & Gallimore 1989; Kutzbach 1994). Namely, the large continents lead to the development of large seasonal temperature extremes, with very warm summers and cold winters, and strong summer and winter monsoon circulations. The distribution of precipitation is controlled by the monsoon circulations in the summer hemisphere and by middle-latitude storm track precipitation in the winter hemisphere. The subtropical continental interiors are arid to semi-arid, being far removed from oceanic moisture sources.

While there is general agreement with previous experiments, the more realistic asymmetric distribution of land with the southern continent larger than the northern continent causes somewhat higher amplitude seasonal cycles on the southern continent.

The presence of mountain and plateaus in this simulation, compared to previous experiments, alters the climate significantly. Heavy precipitation occurs around and over the east–west belt of high elevation just north of the equator and along coastal ranges with upslope flow. Moreover, the general intensity of the monsoon circulation is increased. As a result, summer monsoon precipitation extends somewhat farther into the continent in the LP and LP/EL simulations compared to earlier results (Kutzbach 1994; Kutzbach & Gallimore 1989).

Table 1 summarizes the average precipitation for the globe (land and ocean), land and ocean for these experiments, for a previous experiment with idealized Pangean geography and no mountains, and for a modern (control) experiment. The idealized Pangean simulation (Kutzbach 1994) had less precipitation over land than the experiment with modern geography, owing to the more arid interior of the supercontinent. In the LP and LP/EL experiments, the presence of topographic features on the continents significantly increased the overall precipitation over land by about 25% compared to the idealized Pangea case. The increased CO_2 level and higher temperatures of the LP, LP/EL and idealized Pangean experiments caused a generally high precipitation rate. Thus two competing effects, more arid supercontinents but overall increased precipitation related to greenhouse warming partially balanced each other in the global average.

(*e*) *Calibration of climate–biome distribution*

To begin to assess the accuracy of the climate model simulation, we compared the biome distribution for the Late Permian, as estimated by Ziegler (1990) using the biome concepts of Walter (1984), with the

PHILOSOPHICAL TRANSACTIONS OF THE ROYAL SOCIETY B BIOLOGICAL SCIENCES

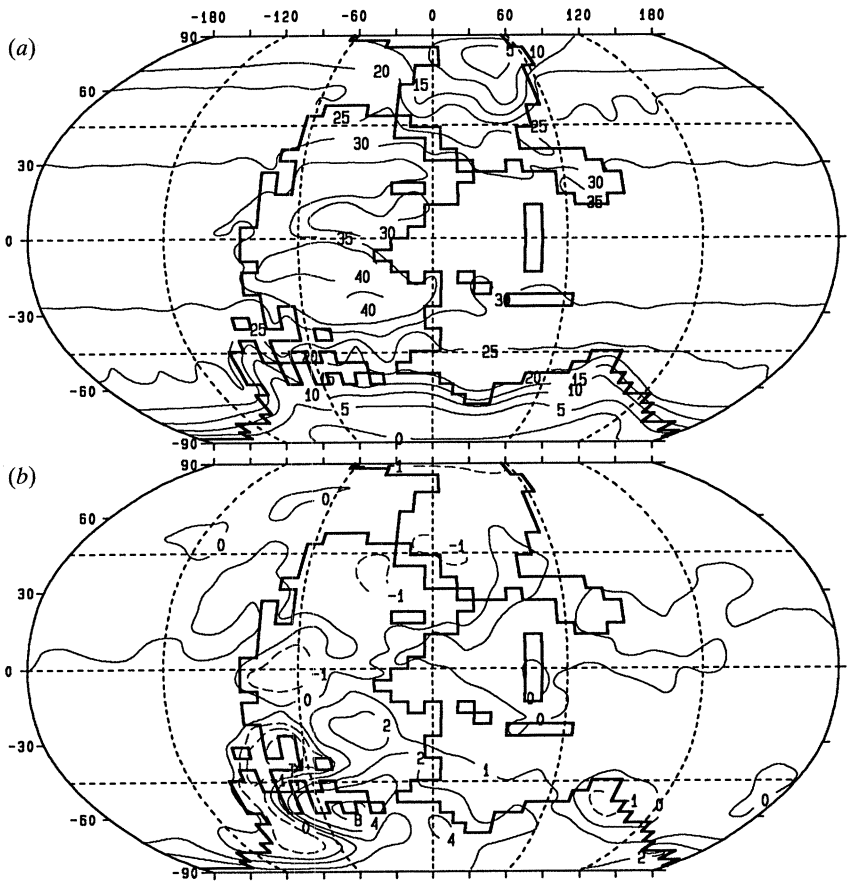

Figure 6. Annual surface temperature (°C) for (*a*) simulation LP/EL and (*b*) the difference, LP/EL minus LP.

climate–biome distribution predicted to be consistent with the results from the climate model. To predict the climate–biome distributions from the output of the climate model, we first described the present-day Walter climate–biome distribution in terms of the seasonal distribution of precipitation and temperature (table 2). The two fundamental criteria used to classify the climates–biomes are counts of the number of months with average temperature equal to or exceeding 5°C (corresponding to sufficient warmth for growth) and the number of months with 40 mm or more of precipitation. The criteria of '5°C' and '40 mm' were arrived at by trial-and-error approximations but are broadly consistent with Walter's more qualitative climate–biome classification and with the rules for the Koeppen classification (Guetter & Kutzbach 1990; Walter 1984). Two additional criteria were found to be necessary to help distinguish between climates–biomes 1 and 5 and climates–biomes 2 and 4, and between climate–biome 4 and climate–biome 5 ; see table 2. Using these classification rules (table 2), we were able to reproduce the general features of the

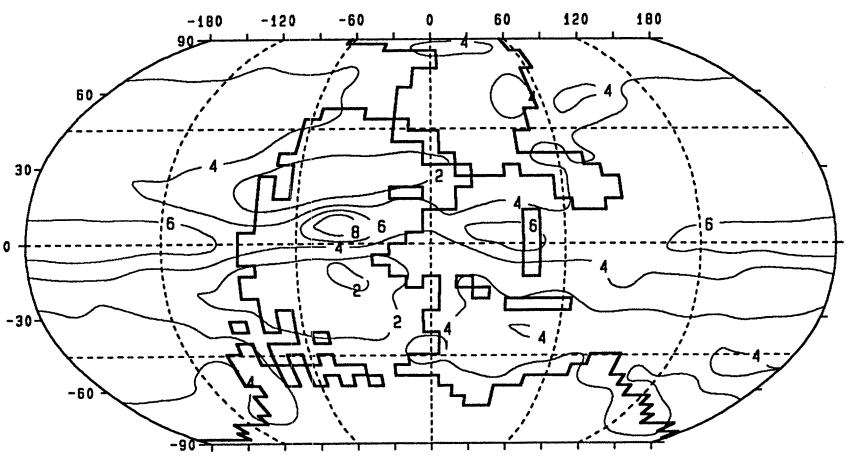

Figure 7. Annual precipitation rate (mm d^{-1}) for simulation LP/EL.

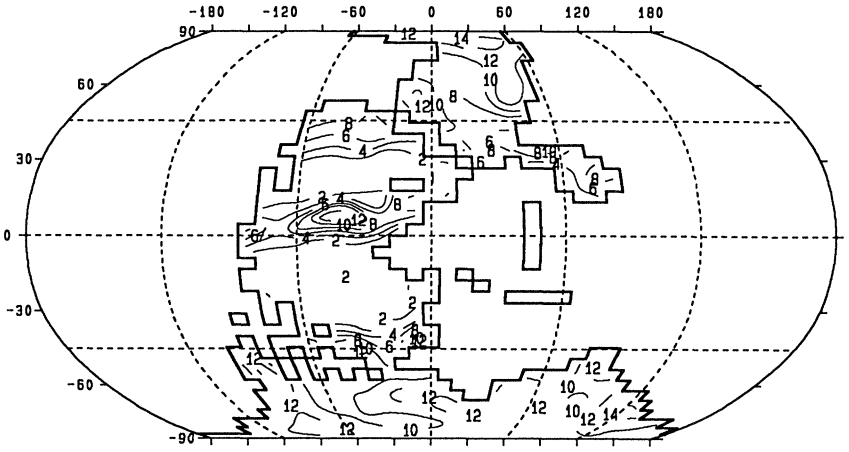

Figure 8. Annual soil moisture (cm) for simulation LP/EL.

present-day Walter climate–biome distribution at the scale of the model's grid (4.4° latitude by 7.5° longitude).

(*f*) *Climate–biome distributions for LP and LP/EL*

The climate–biome distributions for LP (not shown) and LP/EL (figure 9*a*) are similar except in the region of the southern lakes that were included in the LP/EL simulation. The generally similar features of the two simulations are: climates–biomes 1 and 2 occur in much of the tropics and subtropics, except 2a and 3 occur in parts of the tropical and subtropical interiors. Climates–biomes 5 and 6 occur in middle latitudes (40–60° latitude) and in the tropics at higher elevations and climate–biome 8 is found in polar latitudes. The presence of the extensive southern lakes in LP/EL significantly alters the climate–biome distribution compared with LP in several locations (figure 9*a*). Along the southern borders of the lake region where the presence of the lakes made the winters significantly warmer, and farther to the east where warming occurred due to the altered circulation, climates–biomes switched from 8 (LP) to 6 (LP/EL) or from 6 to 5. Along the northern border of the lake region the classes switched from 5 to 1 (temperate to tropical) due to the warmer winters and from 2a to 3 due to decreased rainfall. Farther equatorward along the west coast, the classes switched from 3 to 2a.

Table 1. *Annual-average precipitation (mm) for three climate model experiments: the Late Permian with extensive lakes (LP/EL), an idealized Pangea with no topography (Kutzbach 1994), and a modern control*

(The global-scale averages for simulation LP (not shown) are almost identical to those for LP/EL shown below. Values are for the global average (L + O; land plus ocean), land (L) and ocean (O).)

experiment	L + O	L	O
LP/EL	1420	1170	1520
idealized Pangea	1200	925	1360
modern	1220	1190	1240

The simulated climate–biome distribution (figure 9*a*) agrees reasonably well with the observations summarized by Ziegler (1990): figure 9*b*. Areas of agreement include the location of classes 8, 6, 5 and 1 in eastern Laurasia, 3 in western Laurasia and western Gondwana (note that both the numerals 3 and 7 and the stippled areas in figure 9*b* indicate aridity), and 5 and 6 across middle latitudes of Gondwana. The agreement across the middle latitudes of Gondwana is significantly better with LP/EL (figure 9*a*) than with LP because, as mentioned above, many locations switched from 8 (LP) to 6 (LP/EL) along the southern borders of the lake region. An area of disagreement is the high latitude region of Gondwana, south of 60° S, where the model indicates climate–biome 8 and the observations indicate climate–biome 6. Truswell (1991) has commented that '. . . the Antarctic macrofossil floras of the Permian are poor in numbers of taxa when compared with coeval plant assemblages from other Gondwana continents', so a cold temperate biome 8 may very well be indicated. Another area of disagreement is central Laurasia, along the seaway, where the model indicates climate–biome 2 and the observations indicate climate–biome 3.

5. CONCLUSIONS

These simulations for the Late Permian have more realistic prescriptions of land–ocean boundaries, topography, and inland lakes and seas than some previous simulations of supercontinents with idealized boundaries and no topographic features. The simulated climate retains a general agreement with previous results but also includes major and significant differences. The items of general agreement include the large extremes of temperature (hot summers, cold winters), the arid subtropical interiors, and the strong monsoonal circulations bringing summer precipitation to tropical and subtropical east coasts.

The major differences between these and previous simulations can be traced to the roles of topography and the presence of inland lakes and seas. The east–west mountain range north of the equator is a focal point for precipitation in all seasons and produces a

Table 2. (*a*) *Walter climates and biomes*

number	climates	biomes
1	tropical, humid	tropical rain forest
2	tropical, humid summers	tropical deciduous forest
2a	tropical, semi humid	savanna
3	subtropical, arid	desert
4	warm temperate, dry summers	sclerophyllous woody plants
5	warm temperate, humid	temperate evergreen forests
6	cool temperate	nemoral broadleaf deciduous forests
7	cool temperate, dry summers	steppe
7a	cool temperate, arid	desert
8	cold temperate	boreal coniferous forests
9	polar	tundra
I	ice	—

Table 2. (*b*) *Classification table, showing Walter climates and biomes (by number, see (a) above) as a function of the number of months with temperatures of 5°C or more, and the number of months with 40 mm or more of precipitation*

(An additional criterion was added to help distinguish between tropical biomes 1 and 5, and biomes 2 and 4. If the number of months having temperatures greater than 5°C was 12, but the 'growing season degree months', or GSDM, was less than the adjustable parameter '$GSDM_0$', the second row of the translation table was used, instead of the first. 'Growing season degree months' was defined as (mean monthly temperature -5), summed over all months in the year. After experimentation, $GSDM_0$ was set at 225 degree months. This additional criterion was needed because both tropical and temperate climates–biomes may have all months well above 5°C, yet temperate climates–biomes have 'winters' that may drop to, say, 15°C whereas tropical climates–biomes stay evenly warm. For example, for a humid region that has 12 months >5°C: if the temperature is 25°C each month then 'GSDM' is $(25-5)\times 12=240$ and it is classified biome 1; however, if the temperature drops to, say, 15°C for 3 months then 'GSDM' is $(25-5)\times 9+(15-5)\times 3=210$ and it is classified climate–biome 5. To further distinguish between climate–biome 4 (warm temperate, dry summers or 'Mediterranean') and climate–biome 5 (warm temperate, humid), we used the Koeppen criterion, that for Mediterranean climates (Cs, summer drought) the rainfall of the wettest winter month is at least three times that of the driest summer month. For example, if the two primary criteria identified a region as climate–biome 4, then the above mentioned criterion on summer versus winter rain is applied to either confirm the classification or change it from 4 to 5.)

number of months having 40 mm or more of precipitation													number of months with temperatures
0	1	2	3	4	5	6	7	8	9	10	11	12	>5°C
3	3	3	3	2a	2	2	2	2	2	1	1	1	12
3	3	3	3	3	4	4	4	4	4	5	5	5	11[a]
7a	7a	7a	7	7	4	4	4	4	5	5	5	5	10
7a	7a	7	7	7	5	5	5	5	5	5	5	5	9
7a	7a	7	7	7	5	5	5	5	5	5	5	5	8
7a	7a	7	7	7	6	6	6	6	6	6	6	6	7
7a	7a	7	7	7	8	8	8	8	8	8	8	8	6
7	7	8	8	8	8	8	8	8	8	8	8	8	5
7	7	8	8	8	8	8	8	8	8	8	8	8	4
7	7	8	8	8	8	8	8	8	8	8	8	8	3
9	9	9	9	9	9	9	9	9	9	9	9	9	2
9	9	9	9	9	9	9	9	9	9	9	9	9	1
I	I	I	I	I	I	I	I	I	I	I	I	I	0

[a] Or 12 and $GSDM<GSDM_0=225$.

much wetter tropical climate than exists in simulations without these mountains. The mountains and plateaus of the subtropical and lower middle latitudes became the locations of the centres of lowest pressure for the summer monsoons of both hemispheres. The presence of these highlands also serves to intensify the monsoons, compared with previous simulations, in much the same way that the presence of the Tibetan Plateau intensifies the South Asian monsoon. The intensified monsoons draw precipitation somewhat farther into the continent than in previous idealized Pangean simulations. The presence of coastal mountains in middle latitudes causes upslope winds that enhance onshore precipitation.

The presence of inland lakes and seas in the middle latitudes of Gondwana in one simulation (LP/EL) causes large regional climatic differences compared to the simulation that omits these bodies of water (LP). The summers are not as hot and the winters not as cold and the overall amplitude of the seasonal cycle of

PHILOSOPHICAL TRANSACTIONS OF THE ROYAL SOCIETY B BIOLOGICAL SCIENCES

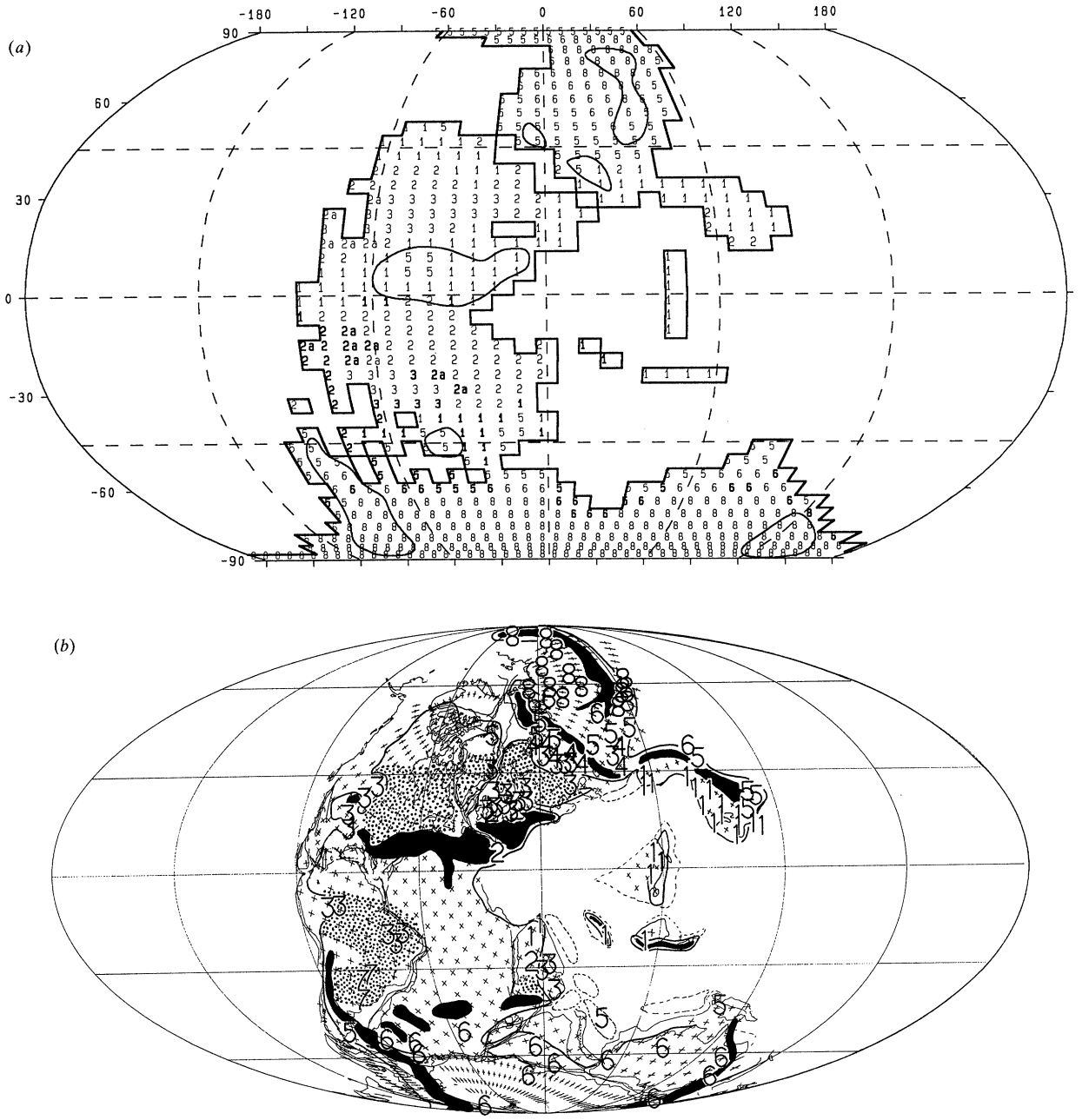

Figure 9. Walter climate–biome classification for (*a*) simulation LP/EL, and (*b*) observations summarized by Ziegler (1990). The closed lines in (*a*) mark the 1000 m elevation contour. The Southern Hemisphere climates–biomes that changed in simulation LP/EL, compared with LP, are identified with bold numerals. In (*b*), the areas of dark shading represent highlands and the areas of stipple indicate aridity. See table 2*a* for description of climates–biomes.

temperature is reduced by a factor of two. Although the largest changes occur in the vicinity of the lakes some effects extend considerably to the east of the lake region. These effects are due to the dynamical response of the circulation to changes in the low-level heating of the atmosphere. In winter, a cyclonic circulation develops and areas to the east of the lakes are warmed by increased poleward flow. In summer, the large lake region reduces the strength of the summer monsoon and shifts its centre, thereby altering rainfall, cloud cover, and temperature over a large area north and east of the lakes. This simulation of a relatively mild climate in the region of lakes and seas is in accord with the diverse tetrapod faunas of the southern Africa region (Yemane 1993).

The use of the Walter classification of climates and biomes allowed us to compare the simulation of the Late Permian with observations of Late Permian vegetation that had been summarized using Walter's biome concepts. The agreement between the model and the geologic data was very good in many areas, poor in two areas, and uncertain in several areas where observational evidence is scarce (see previous section).

These specific results could be modified further depending upon changes in the choice of land–ocean boundaries, topography, inland lakes and seas, and CO_2 level for Late Permian time. Such changes are to be expected for two reasons. First, our knowledge of past conditions will improve and second, our ability to incorporate these conditions in models will improve as the model resolution improves. For example, the spatial resolution of the model used in these experiments is too coarse to account properly for all of the effects of topography and large lakes and seas on climate. Because of the coarse resolution of this model, the area of inland lakes and seas had to be somewhat exaggerated to incorporate their effects. At a later stage the depth of these bodies of water might also need to be specified more accurately.

The model used here has significant limitations in its ability to simulate the present climate and therefore the estimates of past climate and past biomes are also subject to error. The lack of an interactive dynamical ocean as part of the climate model is a very significant limitation. These kinds of experiments should be repeated using models with interactive oceans when such calculations with high resolution coupled atmosphere–ocean models are feasible. The lack of an interactive vegetation model is also a significant limitation. Using an interactive vegetation model would avoid the necessity of prescribing the land albedo.

The classification scheme for translating the output of the climate model into Walter classes of climates and biomes is a useful first step that worked reasonably well at the coarse spatial resolution of the climate model. However, the parameters and criteria used in the classification are not necessarily the optimum choices and considerable work could be undertaken to improve the classification particularly for applications to higher resolution data sets.

The agreements found in the present study between model simulations and floral assignments of climates through the Walter biome classification are encouraging, but much will be done in the near future to achieve a more objective treatment of the floral data. Taxonomic lists from many more regions have been assembled, and will be subjected to statistical tests to determine floral gradients. Previously, the provinces proposed by palaeobotanists over the years were accepted and assigned to the most appropriate modern biome (Ziegler 1990). In reality, the floras, like the climates, are gradational in nature, so statistical ordination tests are being designed to help choose the biome boundaries in a uniform manner. So, some 'fine-tuning' will be required before a detailed comparison of the model and floral determinations will be justified. Circularity will be avoided by careful attention to the physiognomic adaptations of the plants and animals. Also the model can be tested against the palaeontologic evidence to see if the boundaries are parallel and consistent on a global basis.

A research grant to the University of Wisconsin-Madison from the National Science Foundation, Climate Dynamics program, supported the modeling work; the grant number is ATM 89–02849. The climate model computations were made at the National Center for Atmospheric Research (NCAR), which is sponsored by the National Science Foundation, with computing grant 35381017 from the NCAR computing facility. The authors thank Peter Guetter for running the climate model experiments and calculating the Walter climate–biome distributions, Pat Behling and Rich Selin for statistical summaries and graphics, Mary Kennedy for manuscript preparation, and Brian Hoskins and another reviewer for comments and suggestions.

REFERENCES

Berner, R.A. 1990 Atmospheric carbon dioxide levels over Phanerozoic time. *Science, Wash.* **249**, 1382–1392.

Covey, C. & Thompson, S.L. 1989 Testing the effects of ocean heat transport on climate. *Paleogeor. Paleoclim. Paleoecol.* **75**, 331–334.

Crowley, T.J. & Baum, S.K. 1992 Modeling late Paleozoic glaciation. *Geology* **20**, 507–510.

Crowley, T.J., Mengel, J.G. & Short, D.A. 1987 Gondwanaland's seasonal cycle. *Nature, Lond.* **329**, 803–807.

Crowley, T.J. & North, G.R. 1991 *Paleoclimatology*. New York: Oxford University Press.

Crowley, T.J., Short, D.A., Mengel, J.G. & North, G.R. 1986 Role of seasonality in the evolution of climate over the last 100 million years. *Science, Wash.* **231**, 579–584.

Guetter, P.J. & Kutzbach, J.E. 1990 A modified Köppen classification applied to model simulations of glacial and interglacial climates. *Clim. Change* **16**, 193–215.

Hoskins, B.J. & Karoly, D.J. 1981 The steady linear response of a spherical atmosphere to thermal and orographic forcing. *J. atmos. Sci.* **38**, 1179–1196.

Hunt, B.G. 1979 The influence of the Earth's rotation rate on the general circulation of the atmosphere. *J. atmos. Sci.* **36**, 1392–1408.

Kutzbach, J.E. 1994 Idealized Pangean climates: sensitivity to orbital change. In *Pangea: paleoclimate, tectonics and sedimentation during accretion, zenith, and breakup of a supercontinent*. (ed. G. Klein). Boulder, Colorado: Geological Society of America, Special Paper 288.

Kutzbach, J.E. & Gallimore, R.G. 1989 Pangaean climates: megamonsoons of the megacontinent. *J. geophys. Res.* **94**, 3341–3357.

Kutzbach, J.E., Guetter, P.J. & Washington, W.M. 1990 Simulated circulation of an idealized ocean for Pangaean time. *Paleoceanography* **5** (3), 299–317.

Pitcher, E.J., Malone, R.C., Ramanathan, V., Blackmon, M.L., Puri, K. & Bourke, W. 1983 January and July simulations with a spectral general circulation model. *J. atmos. Sci.* **40**, 580–604.

Randel, W.J. & Williamson, D.L. 1990 A comparison of the climate simulated by the NCAR Community Climate Model (CCM1:R15) with ECMWF analyses. *J. Climate* **3**, 608–633.

Scrutton, C.T. 1978 Periodic growth features in fossil organisms and the length of the day and month. In *Tidal friction and the Earth's rotation* (ed. P. Brosche & J. Sündermann), pp. 154–196. Berlin: Springer-Verlag.

Truswell, E.M. 1991 Antarctica: a history of terrestrial vegetation. In *The geology of Antarctica* (ed. R. J. Tingey), pp. 499–537. Oxford: Clarendon Press.

Walter, H. 1984 *Vegetation of the Earth and ecological systems of the geobiosphere*, 3rd edn. Berlin: Springer-Verlag.

Williams, G. P. 1985 Jovian and comparative atmospheric modeling. *Adv. Geophys.* **28A**, 381–429.

Yemane, K. 1993 Contribution of Late Permian paleogeography in maintaining a temperate climate in Gondwana. *Nature, Lond.* **361**, 51–54.

Ziegler, A.M. 1990 Phytogeographic patterns and continental configurations during the Permian Period. In *Palaeozoic palaeogeography and biogeography* (ed. W. S. McKerrow & C. R. Scotese), pp. 363–379. Boulder, Colorado: Geological Society of America.

Ziegler, A. M. 1993 Models come in from the cold. *Nature, Lond.* **361**, 16–17.

PHILOSOPHICAL TRANSACTIONS OF THE ROYAL SOCIETY B BIOLOGICAL SCIENCES